DEUTSCHES ELEKTRONEN-SYNCHROTRON DESY

DESY 75/43
October 1975

A Model for the Process $e^+e^- \to \rho^0\varepsilon$

by

F. Gutbrod
Deutsches Elektronen-Synchrotron DESY, Hamburg

U. Weiss
Institut für Theoretische Physik der Universität Stuttgart

2 HAMBURG 52 · NOTKESTIEG 1

To be sure that your preprints are promptly included in the
HIGH ENERGY PHYSICS INDEX ,
send them to the following address (if possible by air mail) :

A Model for the Process $e^+e^- \to \rho^0\varepsilon$

by

F. Gutbrod

Deutsches Elektronen-Synchrotron DESY, Hamburg, Germany

and

U. Weiss

Institut für Theoretische Physik

der Universität Stuttgart, Germany

Abstract

We have calculated the $\rho\varepsilon\gamma$ form factors in the timelike region from simple loop diagrams. The results for the cross section $e^+e^- \to 2\pi^+ 2\pi^-$ depend crucially on the model for the pion form factor. If $\rho\varepsilon$ - intermediate states are neglected there, the calculated cross sections fall much below the data. If these states are included and the existence of a ρ'-meson is assumed, the data are explained correctly.

I. Introduction

In two experiments [1,2] at ADONE, Frascati, a large cross section in the order of 20 nb has been found for the reaction

$$e^+e^- \to 2\pi^+2\pi^- \tag{1.1}$$

around $\sqrt{s}$ = 1.5 GeV ($\sqrt{s}$ = e^+e^- c.m.-energy). A similar enhancement is established in the process

$$\gamma p \to 2\pi^+2\pi^- p \tag{1.2}$$

at 9.3 GeV photon energy [3]. Up to now it is not completely evident that the observed s-behaviour is due to an existence of a ρ'resonance. The $\pi\pi$-phase shift analysis is still ambiguous in this region, and the electromagnetic pion form factor is, because of lack of statistics [5], not determined well enough there to draw conclusions about possible resonant behaviour. A nonresonant interpretation of the observed peak in (1.1) as due to the $\rho^o\varepsilon$ channel coupled to the tail of the ρ-meson has been given by Kramer and Hirshfeld [6], where one of the $\gamma\rho\varepsilon$ coupling constants is taken, after a Vector Dominance extrapolation, from calculations of the $\varepsilon\gamma\gamma$-vertex [7].

Assuming that the reaction (1.1) is indeed dominated by the quasi two body reaction

$$e^+e^- \to \rho^o\varepsilon\ , \tag{1.3}$$

it is natural to try to calculate the corresponding amplitudes from triangle diagrams with low mass intermediate particles, such as in fig. 1a) and 1b). Here the blobs denote renormalized vertex functions, and the propagators are taken as dressed ones. The electromagnetic $\pi\pi$- and $\pi\omega$-vertices of course contain the ρ-pole. Recently [8] we have worked out a field theoretic model for these vertices, which also determines the pion propagator via the Ward identity[+]. From this model also the $\rho\pi\pi$ vertex and the $\rho\pi\omega$ vertex can be derived, which appear in fig. 1. The $\varepsilon\pi\pi$ vertex however is unknown except onshell (as determined by $\Gamma_{\varepsilon\pi\pi}$) and we have to make simple guesses. We note that due to the $\rho\pi\pi$ and $\varepsilon\pi\pi$ vertex functions the triangle diagrams are not divergent.

The diagram 1a) taken alone would not lead to a conserved current, and it must be supplemented by diagrams where the photon couples not to pions. For a ρ-meson without internal structure (with a constant $\rho\pi\pi$ vertex) a contact term is needed as in QED for scalar mesons. If one adopts a Bethe-Salpeter model of the ladder type as in I, one has to couple the photon to the internal lines of the ρ-constituents, which are nucleon lines in our model. Since the nucleons are not pointlike, such quasi contact diagrams are s-dependent, i.e. have form factors, in agreement with recent observation [9]. We have analyzed the s-dependence of such diagrams (see fig. in sect. III) and then replaced it by simpler diagrams. The overall normalization of the contact term is then derived from the required

[+] Ref. [8] will be quoted as I henceforth.

absence of kinematical singularities of one form factor in the following way. According to Kramer and Walsh [10] we write for the ρε current matrix element

$$\langle k_\rho k_\varepsilon | j_\mu(0) | 0 \rangle = F^{(1)}_{\rho\varepsilon\gamma}(s)\left(e^*_\mu s - q_\mu e^*\cdot q\right) + F^{(2)}_{\rho\varepsilon\gamma}(s)\left(e^*_\mu k_\varepsilon\cdot q - k_{\varepsilon\mu} e^*\cdot q\right) \tag{1.4}$$

Here e_μ denotes the ρ polarisation vector and $q_\mu\,(k_{\varepsilon\mu})$ the photon (ε) four momentum. According to perturbation theory the form factors $F^{(1)}_{\rho\varepsilon\gamma}(s)$ and $F^{(2)}_{\rho\varepsilon\gamma}(s)$ are free of kinematical singularities, since the elimination of a third form factor via current conservation does not create new singularities. We alternatively can express the current matrix element by helicity amplitudes $\Gamma_{\lambda_\rho}(s)$

$$\langle k_\rho, \lambda_\rho, k_\varepsilon | j_{\lambda_\gamma} | 0 \rangle = \mathcal{D}^{1*}_{\lambda_\gamma,\lambda_\rho}(\phi, \vartheta, -\phi)\,\Gamma_{\lambda_\rho}(s) \tag{1.5}$$

with the ρ helicity $\lambda\rho = 0, 1$, and the ρ angles ϑ, ϕ are taken relative to the beam axis. Then from the relations [10] (m = ρ-mass = ε-mass)

$$F^{(1)}_{\rho\varepsilon\gamma}(s) = \frac{2}{s-4m^2}\left[\frac{s-2m^2}{s}\Gamma_1(s) - \frac{m}{\sqrt{s}}\Gamma_0(s)\right], \tag{1.6}$$

$$F^{(2)}_{\rho\varepsilon\gamma}(s) = \frac{2}{s-4m^2}\left[\frac{2m}{\sqrt{s}}\Gamma_0(s) - \Gamma_1(s)\right]$$

one sees that

$$\Gamma_1(0) = 0 . \tag{1.7}$$

We shall achieve this by the normalization of the contact diagram.

In I we were restricted in the s-region, where the $\pi\pi$-Bethe-Salpeter equation could be solved numerically. This came through the anomalous singularities in the dispersion representation of $\rho\varepsilon$-loops with a $\pi\pi$-state in the t-channel. Consequently we had to extrapolate the pion form factor $F_\pi(s)$ with a generalized effective range expansion into the time-like region with $s > m_\rho^2$. The $\rho\varepsilon$-form factors however have more complicated analytic properties than $F_\pi(s)$ due to the large ρ- and ε-masses. These lead both to anomalous thresholds [+)] in s and to integration contour distortions in the momentum integrals corresponding to fig. 1a) and 1b). We have eliminated these difficulties by making the external ρ- and ε-masses s dependent, such that they agree at a point in the physical region $s > 4\ m^2$ with the physical ones. It is easy to choose the s-dependence such that no anomalous cuts in s appear, and the extrapolation in s is not too difficult. The calculated cross section for the process (1.3) depends on our model for $F_\pi(s)$. If no $\rho\varepsilon$-loops are included in $F_\pi(s)$, i.e. if $\rho\varepsilon$-unitarity is not taken into account, our extrapolated form factors are much too small to account for the experimental results. If however the $\rho\varepsilon$ loops are included, the form factors are much larger than in the former case. The extrapolated values are however rather unstable to technical details of the extrapolation.

+) An extensive discussion of the analytic structure of $\Gamma_i(s)$ has been given by G. Köpp (to be published)

If we impose, in the extrapolation, the existence of a ϱ' resonance with $m_{\varrho'}$ = 1600 MeV and $\Gamma_{\varrho'}$ = 400 MeV, we achieve stability of the extrapolation and agreement with the data within the (large) experimental errors.

Sect. 2 contains the formulas corresponding to the loops of fig. 1a) and 1b). In sect. 3 we describe the evaluation of the contact term, and the results for the $\varrho\varepsilon$ form factors are displayed in sect. 4. Conclusions are drawn in sect. 5.

II. The $\pi\pi$- and the $\pi\omega$-loops

In this section we consider the contribution of the diagrams fig. 1a) and 1b) to the $\varrho\varepsilon\gamma$ helicity amplitudes, which we call $\Gamma_0^L(s)$ and $\Gamma_1^L(s)$. If we denote, more generally, the two particle irreducible transition amplitudes (or kernels) in the I = J = 1 state for $\pi\pi \to \varrho\varepsilon$ and $\pi\omega \to \varrho\varepsilon$ by $M_\pi(k_1^2, k_2^2, \lambda_\varrho)$ and $M_\omega(k_1^2, k_2^2, \lambda_\varrho)$ resp., we have

$$\Gamma^L_{\lambda_\varrho}(s) = \frac{1}{4\pi^3}\int_{-1}^{+1} d\cos\alpha \sin\alpha \int_0^\infty dk\, k^3 \Big[M_\pi(k_1^2, k_2^2, \lambda_\varrho)\Delta'_\pi(k_1^2)\Delta'_\pi(k_2^2) \times 2|\vec{k}_1| F_\pi(s, k_1^2, k_2^2) + \\ + M_\omega(k_1^2, k_2^2, \lambda_\varrho)\Delta'_\pi(k_1^2)\Delta'_\omega(k_2^2)|\vec{k}_1|\sqrt{s}\, F_{\pi\omega\varrho}(s, k_1^2, k_2^2)\Big]. \tag{2.1}$$

The kinematics is as follows [+]:

$$\begin{aligned} k_{10(20)} &= \frac{\sqrt{s}}{2} \pm i k \cos\alpha \\ |\vec{k}_1| &= |\vec{k}_2| = k \sin\alpha \\ k_{\varrho 0} &= k_{\varepsilon 0} = \frac{\sqrt{s}}{2} \\ |\vec{k}_\varrho| &= |\vec{k}_\varepsilon| = \sqrt{s/4 - m^2}\,. \end{aligned} \tag{2.2}$$

[+] Throughout we put

$$m_\varrho = m_\varepsilon = m\,.$$

By $\Delta'_\pi(k^2)$ we denote the dressed pion propagator taken from I, and the scalar part of the ω-propagator $\Delta'_\omega(k^2)$ is taken equal to the pion propagator. The form factors $F_\pi(s,k_1^2,k_2^2)$ and $F_{\pi\omega\gamma}(s,k_1^2,k_2^2)$ also follow from I. The integration contour for k and $\cos\alpha$ may in fact be more complicated than indicated in (2.1) (see sect. 3). If the kernels are approximated by one pion exchange, we find, including a factor 2 for two possible diagrams of fig. 1a:

$$M_\pi(k_1^2, k_2^2, \lambda_\gamma = 0) = 2\sqrt{s}\, g_{\gamma\pi\pi} g_{e\pi\pi} \Big[\tfrac{1}{3} |\vec{k}_1| \big(\bar{Q}_0(k_1,k_\gamma) + 2\,\bar{Q}_2(k_1,k_\gamma)\big) - |\vec{k}_\gamma|\,\bar{Q}_1(k_1,k_\gamma)\Big] \tag{2.3}$$

$$M_\pi(k_1^2, k_2^2, \lambda_\gamma = 1) = 4m\, g_{\gamma\pi\pi} g_{e\pi\pi}\, \tfrac{1}{3} |\vec{k}_1| \big(\bar{Q}_0(k_1,k_\gamma) - \bar{Q}_2(k_1,k_\gamma)\big) \tag{2.4}$$

$$M_\omega(k_1^2, k_2^2, \lambda_\gamma = 0) = 2\,\frac{m^2}{m_\omega}\, g_{\gamma\pi\omega} g_{e\pi\pi}\, \tfrac{1}{3} |\vec{k}_1| \big(\bar{Q}_0(k_1,k_\gamma) - \bar{Q}_2(k_1,k_\gamma)\big) \tag{2.5}$$

$$M_\omega(k_1^2, k_2^2, \lambda_\gamma = 1) = \frac{\sqrt{s}\,m}{2\,m_\omega}\, g_{\gamma\pi\omega} g_{e\pi\pi} \Big[\tfrac{1}{3} |\vec{k}_1| \big(2\bar{Q}_0(k_1,k_\gamma) + \bar{Q}_2(k_1,k_\gamma)\big) - |\vec{k}_\gamma|\,\bar{Q}_1(k_1,k_\gamma)\Big(1 - \frac{2ik\cos\alpha}{\sqrt{s}}\Big)\Big] \tag{2.6}$$

We have abbreviated

$$\bar{Q}_\ell(k_1,k_\gamma) = -\tfrac{1}{2}\int_{-1}^{+1} dz\, P_\ell(z)\, \Delta'_\pi\big((k_1-k_\gamma)^2\big)\, \Gamma_\gamma(k_1,k_\gamma)\, \Gamma_\ell(k_2,k_e) \tag{2.7}$$

with $\qquad z = \cos(\vec{k}_1, \vec{k}_\gamma)$.

For pointlike vertices and a free propagator, $2|\vec{k}_1||\vec{k}_3|\,\bar{Q}_\ell(k_1,k_3)$ reduces to a Legendre function of second kind. The $\rho\pi\pi$- and the $\rho\pi\omega$ vertex functions follow from our model I (they are roughly equal), whereas the $\varepsilon\pi\pi$-vertex function is unknown. We assume it to be equal to $\Gamma_\rho(k_1,k_3)$.

As discussed in I, our method for solving the BSE for $F_\pi(s)$ works only in the region (μ = pion mass)

$$(\sqrt{s}-\mu)^2 \leq m^2+\mu^2 \tag{2.8}$$

since for larger values of s the dispersion relations for the $\rho\varepsilon$-loop inside the pion f.f. would develop anomalous thresholds. Therefore we again have to calculate the helicity amplitudes $\Gamma_i^L(s)$ in the same region with high accuracy and extrapolate them to the physical region $s > 4m^2$. In the region (2.8) however the singularities of the pion propagator in (2.3) - (2.6) lead to a logarithmic singularity in the integration variable α at

$$\sin\alpha = \pm\frac{k^2+\mu^2+\frac{s}{4}-m^2-i\varepsilon}{2k\sqrt{s/4-m^2}}\,. \tag{2.9}$$

These singularities require a deformation of the k-integration into the complex plane [+)] in the unphysical region (2.8). We have circumvented this

[+)] These difficulties are intimately connected with the anomalous singularities of the form factors $F^{(i)}_{\rho\varepsilon\rho}(s)$ as functions of s.

difficulty by making the external ρ and ε mass s-dependent:

$$m^2 \to m^2(s) = \frac{s}{s_p}(m^2 + 2\mu^2) - 2\mu^2 \qquad (2.10)$$

with $s_p > 4m^2$.

Thus our extrapolated amplitudes agree only at the point $s = s_p$ with the physical ones. By this substitution the anomalous thresholds disappear, and no other singularities are introduced, as it is evident from the Nakanishi representation [11] of the vertex with two equal masses:

$$\Gamma(s, m^2) = \int_0^1 d\beta \int_{\kappa_0(\beta)}^{\infty} d\kappa \frac{\varphi(\kappa, \beta)}{(1-\beta)s + \beta m^2 - \kappa + i\varepsilon} \qquad (2.11)$$

where $4\mu^2 \geq \kappa_0(\beta) \geq 3\mu^2$. With the replacement (2.10) only the normal cut for $s \geq 4\mu^2$ is present.

Before discussing our results, we have to explain the calculation of the contact term in the next section.

III. The contact term

As stated in the introduction, the magnitude of the contact term (i.e. those diagrams necessary to restore gauge invariance) is controlled by (1.7) which follows from current conservation. Therefore we have to calculate the pion loop contribution (2.1) at s = o with the physical external mass m. The

correct analytic continuation of (2.1) from the physical region $s \geq 4\,m^2$ requires a deformation of the k-integration contour. Otherwise one of the singularities of the exchanged pion (2.9) will cross the $\cos\alpha$ -contour for some $k > 0$ and will not return for $k \to \infty$ (we do not consider here the necessary distortions of the $\cos\alpha$ -contour due to the propagator poles in the intermediate pion states). A sufficient deformation is shown in fig. 2. The departure of the k-contour from the imaginary axis is at

$$k = B = -i\sqrt{m^2-\mu^2} \tag{3.1}$$

At this value, for $s = 0$, the singularity (2.9) reaches the real α-axis and is stationary. In order to make the $\cos\alpha$ -integration harmless, we have expanded $\bar{Q}(k_1,k_\varrho)$ into Gegenbauer polynomials in $\cos\alpha$, whereby only the lowest term will survive because of the O(4)-symmetry [12] of the Bethe-Salpeter equation at $s = 0$. Thus the calculation of the pion triangle diagram at $s = 0$ is feasable and the normalization of the contact term is fixed.

For the s-dependence of the contact term we have to rely on Feynman diagram considerations. It is physically clear that the contact term arises from a coupling of the photon to charged constituents of the ϱ- and ε-meson other than pions. If we rely on our resonance model I for the ϱ, the nucleon current will give the most important contribution. The photon coupling to a nucleon running parallel to the pions leads to the triangle diagram of fig. 3a), whereas the coupling to an exchanged nucleon gives the complicated structure of fig. 3b). The nucleon vertices can be taken as dressed ones, since we are working with dressed propagators throughout, but we only consider

the γ_μ-coupling of the photon. The ratio of the two diagrams is impossible to estimate, since the coupling constant $g_{\varepsilon N\bar{N}}$ is poorly known [13], and the calculation of fig. 3b) with vertex corrections etc. is too complicated. We have concentrated our interest on this latter diagram since in view of the large nucleon mass and the small nucleon isovector charge we think it unlikely that diagram 3a) can compensate the contribution of $\Gamma_1(s = o)$ of diagram 1a). An analysis of the spin traces also shows that for[+] $s < 4\ M^2$ the main contribution with respect to the spin structure is, for both diagrams, of the form

$$\langle k_\varsigma, k_\varepsilon \mid j_\mu(o) \mid o \rangle \sim e^*_\mu \cdot f(s) \tag{3.1}$$

in the notion of (1.4). Therefore the neglection of diagram 3a) will not influence the ratio of $\Gamma_0(s)$ and $\Gamma_1(s)$ very much. We have analysed the s-dependence of fig. 3b and its average off-shell momentum of the nucleons, including all spin terms, but with free propagators and bare couplings except for the $\varsigma N\bar{N}$ vertex. This was done with Feynman parameters and numerical integrations. The $\varsigma N\bar{N}$ vertex was simulated by differentiation with respect to adjacent nucleon masses. We found, besides the dominance of the spin structure (3.1), that the energy dependence introduced by the nucleon spin terms is less than 10 % between s = o and s = 4 M^2. We consequently replaced the diagram 3b by the simpler structure of fig. 4a) with scalar particles, the $\gamma\varsigma$ spin structure being given by (3.1). The value of the mass $M_c^2 \approx 5\ M^2$ ensures that the average nucleon off-shell momentum is the same as in fig. 3b). This is necessary to get the correct nucleon off-shell form factor. We have taken into account only the pion current contribution to the nucleon form factor. This leads to the diagram of fig. 4b with a subtraction for the

+) M = nucleon mass.

nucleon vertex:

$$\Gamma^{c}_{\lambda_g}(s) = \frac{Z_1(\hat{k}^2)}{4\pi^3}\int_{-1}^{+1} d\cos\alpha \sin\alpha \int_0^\infty dk\, k^3 \Big\{ M^c(k_1^2, k_2^2, \lambda_g)\Delta'_\pi(k_1^2)\lambda$$

$$\times \Delta'_\pi(k_2^2)|\vec{k}_1|^2 F_{\pi,\,unren.}(s, k_1^2, k_2^2) \qquad (3.2)$$

$$- M^c_{sub}(\lambda_g)\,\bar{Q}_0(\hat{k}, k_1, M^2)\Delta'_\pi(k_1^2)\Delta'_\pi(k_2^2)|\vec{k}_1|^2 F_{\pi,\,unren.}(0, k_1^2, k_2^2)\Big|_{s=0} \Big\}$$

Here we have for the scalar box diagram

$$M^c(k_1^2, k_2^2, \lambda_g = 1) = g_c \int_{-1}^{+1} d\cos\beta \sin\beta \int_0^\infty dq\, q^3 \Delta'_M(P_1^2)\Delta'_M(P_3^2) \times$$

$$\times \bar{Q}_0(P_1, k_g, M_c^2)\bar{Q}_0(P_1, k_1, M^2), \qquad (3.3)$$

$$M^c(k_1^2, k_2^2, \lambda_g = 0) = \frac{\sqrt{s}}{2m} M^c(k_1^2, k_2^2, \lambda_g = 1), \qquad (3.4)$$

$$\bar{Q}_0(P_1, k_g, M_c^2) = -\frac{1}{2}\int_{-1}^{+1} dz\, \Delta'_{M_c}((P_1 - k)^2)\Gamma_g(P_1, k_g)\Gamma_e(P_3, k_e). \qquad (3.5)$$

The propagators $\Delta'_M(P^2)$ and $\Delta'_{M_c}(P^2)$ are dressed propagators with masses M and M_c resp. The kinematics is

$$P_{10(30)} = \mp\frac{\sqrt{s}}{2} - iq\cos\beta, \qquad (3.6)$$

$$|\vec{P}_1| = |\vec{P}_3| = q\sin\beta.$$

The amplitude $M^c_{sub}(\lambda_\rho)$ entering the subtraction term is obtained from (3.3) by omitting $\bar{Q}_o(p_1,k_1,M^2)$. The renormalization constant $Z_1(\hat{k}^2)$ and the subtraction momentum $\hat{k}$ are the same as in I.

The coupling constant g_c is now determined by (see (1.7))

$$\Gamma_1^L(0) + \Gamma_1^c(0) = 0 \quad . \tag{3.7}$$

IV. Extrapolation into the physical region and numerical results

We have worked with the following set of coupling constants:

$$\frac{g^2_{\rho\pi\pi}}{4\pi} = 2.5 \qquad \text{and} \qquad \frac{g^2_{\varepsilon\pi\pi}}{4\pi} = 2.1 \quad . \tag{4.1}$$

The latter value corresponds to $\Gamma_{\varepsilon\pi\pi} = 500$ MeV for $m_\varepsilon = 700$ MeV. The coupling constant $g_{\rho\pi\omega}$ is taken from the width of the ω as [14]

$$\frac{g^2_{\rho\omega\pi}}{4\pi} = 13.8 \quad . \tag{4.2}$$

The sign of $g_{\rho\omega\pi}$ with respect to the other coupling constants is determined by the consideration, that for $s = m_\rho^2$ and vanishing ε four momentum the ε acts as an mass insertion into positive definite ρ self energy diagrams. Thus the s-wave contributions from 1a) and 1b) must have the same sign.

In the actual calculations we have multiplied the diagram 1a) by 3/2

to account for intermediate $K\bar{K}$ pairs, and the diagram 1b) by 2 for the various $\bar{K}K^*$ states. We have also given the exchanged pion an effective mass of $\mu^{-2} = 3\mu^2$ as an average between the π and K-mass. Our results are not very sensitive with respect to this value.

As stated in sect. 2, we have to extrapolate the amplitudes $\Gamma_0^L(s)/\sqrt{s}$ and $\Gamma_1^L(s)$ with variable mass m(s) from the interval $-m_g^2 \leq s \leq m_g^2$ to the physical region. We shall do this with a generalized effective range expansion as in I. However, the extrapolation is complicated by the fact that the pion loop fig. 1a) leads to a very strong variation in s which is not due to the ρ-pole. This is shown in fig. 5, where the ratio of $\Gamma_1^L(s)/F_\pi(s)$ is displayed. Clearly simple vector meson dominance considerations [6] will not work in this model. In order to facilitate the extrapolation, we have introduced comparison amplitudes $\tilde{\Gamma}_0(s)$ and $\tilde{\Gamma}_1(s)$, which are obtained from (2.1) by the replacements

$$\left.\begin{aligned} F_\pi(s,k_1^2,k_2^2) &\Rightarrow \ln\frac{t^2-4M^2}{t^2-2M^2}\Big/\left(1-t^2/10M^2\right) \\ F_{\pi\omega g}(s,k_1^2,k_2^2) &\Rightarrow \frac{1}{6}\ln\frac{t^2-4M^2}{t^2-2M^2}\Big/\left(1-t^2/10M^2\right) \end{aligned}\right\} \qquad (4.3)$$

with $$t^2 = \frac{1}{2}\left(k_1^2+k_2^2\right) - \frac{s}{4} \,. \qquad (4.4)$$

These comparison amplitudes can be calculated in the physical region $s > 4m^2$ by careful numerical integration of (2.1), and they match the ratios $\Gamma_i^L(s)/F_\pi(s)$ rather well. The form (4.3) has been choosen to simulate $F_\pi(o,k_1^2,k_2^2)$ closely.

We now can extrapolate the helicity amplitudes from the interval $-m_g^2 \leq s \leq m_g^2$ with the ansatz

$$\Gamma_0^L(s)/\sqrt{s} = \frac{\sum_{n=0}^{N_a} a_n k_\pi^{2n} + \sum_{n=1}^{N_b} b_n k_\pi^{2n+1} f(k_\pi) + c\,\tilde{\Gamma}_0(s)/\sqrt{s}}{1 + \sum_{n=1}^{N_a'} a_n' k_\pi^{2n} + \sum_{n=1}^{N_b'} b_n' k_\pi^{2n+1} f(k_\pi) + c' k_\omega^3 f(k_\omega)} \tag{4.5}$$

with corresponding forms for $\Gamma_0^C(s)$, $\Gamma_1^L(s)$ and $\Gamma_1^C(s)$.

We have set

$$k_\pi = \sqrt{\frac{s}{4} - \mu^2},$$
$$k_\omega = \frac{1}{2}\sqrt{s - (\mu + m_\omega)^2}, \tag{4.6}$$
$$f(k) = \frac{1}{W} \ln \frac{2k + W}{2k - W - i\varepsilon}.$$

With $N_a = N_b = N_b' = N_c' = 2$ (11 free parameters) we could fit 14 data points with a relative accuracy better than 4.10^{-6}. The extrapolated amplitudes did not change by more than 15 % in the region $\sqrt{s} < 2$ GeV if one of the $N_a \ldots N_b'$ was changed by one (with an important exception to be explained below). We shall discuss the cross section

$$\sigma_{e^+e^- \to g\epsilon} = \frac{1}{3}\pi\alpha^2 \frac{\sqrt{s - 4m^2}}{s^{5/2}} \left(\left| \Gamma_0^L(s) + \Gamma_0^C(s) \right|^2 + 2 \left| \Gamma_1^L(s) + \Gamma_1^C(s) \right|^2 \right) \tag{4.7}$$

for two versions for the pion form factor $F_\pi(s)$. The first one, which is version B of I, has no contributions from long range pion exchange forces

due to the ρε-channel. It gives slightly low values for $F_\pi(s)$ in the region $s > 1$ GeV^2. The second one is essentially the version C of I, but with $g^2_{\rho\pi\pi}\, g^2_{\varepsilon\pi\pi}/16\pi^2 = 5.23$ instead of 3.74 as in I. In the cross section formula (4.7) we have smeared m^2 over the ρ- and ε-width.

1) We show in fig. 6 the results for $\frac{2}{3}\sigma_{e^+e^-\to\rho\varepsilon}$ of the first version as a broken line and compare them with the data of refs. [1] and [2]. It is evident that the theoretical expectation is too low by an order of magnitude. There is no free parameter to adjust except $g^2_{\varepsilon\pi\pi}/4\pi$, which is already close to its upper limit. The s-behaviour is not compatible with experiment. These findings have to be contrasted to those of ref. [6], where a much larger cross section followed from a VDM extrapolation. This extrapolation is probably not justified in view of fig. 5. It is interesting to notice that the contact helicity amplitudes $\Gamma^c_0(s)/\sqrt{s}$ and $\Gamma^c_1(s)$ are roughly proportional to $F_\pi(s)$. Their contribution reduces the amplitudes in the physical region by 1/5. The whole situation changes drastically when we turn to version C.

2) The helicity amplitudes of the second version do not differ very much from the previous case in the region $-m_3^2 \leq s \leq m_3^2$, since the pion vertex $F_\pi(s,k_1^2,k_2^2)$ is only slightly different. The extrapolated values for $\Gamma^L_0(s)/\sqrt{s}$ and $\Gamma^L_1(s)$ however become very unstable with respect to $N_a \ldots N_b$', and sometimes a pole develops. Optimistically one can interpret this in the sense that our model favours a resonance around 2 GeV which couples strongly to ρε but weakly to ππ, since $F_\pi(s)$ is stable and shows no bump (see I). The position of such a resonance cannot be taken from our extrapolation. We therefore <u>impose</u> the existence of the ρ' with [15] $m_{\rho'} = 1600$ MeV and $\Gamma_{\rho'} = 400$ MeV and extrapolate the amplitude

$$\Gamma^L_0(s) \cdot \left(s - s_0 + \gamma\, k_\varepsilon\, f(k_\varepsilon)\right)/\sqrt{s} \qquad (4.8)$$

and similarly for $\Gamma_1^L(s)$, in the notion of (4.6), with $s_o = 2.44\ GeV^2$ and $\gamma = 0.35\ GeV^2$. The extrapolations become now very stable again, and we obtain the full curve in fig. 6 for $\frac{2}{3}\sigma_{e^+e^-\to\rho\varepsilon}$. This curve is in reasonable agreement with the data, but possibly somewhat low above the ρ'. Thus, if we disregard our indications for the existence of a ρ' based on the extrapolation, we are able to calculate the product of coupling constants $g^{(\lambda_\rho)}_{\rho'\rho\varepsilon} \cdot \frac{1}{\gamma_{\rho'}}$ from simple loop diagrams, once the occurrence of a second Breit-Wigner pole in the amplitudes is assumed. Finally we can determine the angular distribution of the ρ with respect to the e^+e^- beam axis as given by

$$\frac{d\sigma}{d\Omega_\rho} = \text{const}\,(1 + b\cos^2\vartheta) \tag{4.9}$$

with

$$b = \frac{|\Gamma_1(s)|^2 - |\Gamma_0(s)|^2}{|\Gamma_1(s)|^2 + |\Gamma_0(s)|^2} . \tag{4.10}$$

We find at $s = m_{\rho'}^2$

$$b = 0.08\ , \tag{4.11}$$

i.e. almost complete isotropy.

V. Conclusions

We have calculated two loop diagrams in which the $\rho\varepsilon$ state is connected to the $\pi\pi$ and the $\pi\omega$ states via one pion exchange. We gave arguments that the diagrams which are necessary to restore gauge invariance have large internal masses, and they are roughly proportional to $F_\pi(s)$. The loops with

pion exchange are not proportional to $F_\pi(s)$, i.e. a simple ϱ-pole will not adequately describe their s-dependence. If we extrapolate the amplitudes without intermediate $\varrho\varepsilon$ loops into the physical region, the storage ring data for the process $e^+e^- \to 2\pi^+ 2\pi^-$ cannot be explained. If the $\varrho\varepsilon$ loops are included in $F_\pi(s,k_1^2,k_2^2)$ and if we impose a Breit-Wigner pole for the ϱ' in the extrapolation function, we can explain the above cross section within the still large experimental uncertainties. These $\varrho\varepsilon$ loops lead also both to distortion of the $\pi\pi$ p-wave effective range plot and to deviations of $F_\pi(s)$ from the ϱ pole formula above 1 GeV as discussed in I. The evidence for a ϱ' from our model of course cannot be convincing. Better techniques for solving the Bethe-Salpeter equation directly at large s are urgently needed.

Our picture for the ϱ' would correspond to a $\varrho\varepsilon$ scattering state with a mixture of s- and d-waves. The s-wave part, i.e. a ϱ plus something radially symmetric with the quantum numbers of the vacuum, has to be confronted with the quark model interpretation [16] of the ϱ' as a radial excitation of the ϱ. The difference is that in our model the fermion-antifermion triplet s-wave content of the ϱ has no nodes in its radial wavefunctions. We do not know a decisive test between these pictures. Our cross sections without a ϱ' are considerably smaller than those obtained by G. Köpp (unpublished) and by a recent "sidewise" dispersion theoretic treatment by G. Kramer, G. Schierholz and K. Sundermeyer [17]. This difference may be due to the presence of vertex functions which are necessary in our approach to avoid divergences.

Acknowledgements

The authors have gained very much from discussions with Dr. G. Köpp and Prof. G. Kramer. One of us (U.W.) is grateful to H. Joos, H. Schopper, K. Symanzik and G. Weber for the kind hospitality extended to him during his stay at DESY. Helpful discussions with G. Hartmann on the k-contour distortion are gratefully acknowledged.

Figure Captions

Fig. 1 a) Pion current contribution to the $\rho\varepsilon$ transition form factors. $F_\pi(s,k_1^2,k_2^2)$ denotes the renormalized electromagnetic off-shell pion vertex.

b) Omega-pion current contribution to the $\rho\varepsilon$ transition form factors. $F_{\pi\omega\gamma}(s,k_1^2,k_2^2)$ denotes the off-shell $\pi\omega\gamma$-vertex.

Fig. 2 The broken line indicates a sufficient deformation of the k-integration contour of eq. (2.1). The point B is at $k = -i\sqrt{m^2-\mu^2}$.

Fig. 3 a) Contact term diagram arising from the photon coupling to constituent nucleons.

b) contact term diagram arising from the photon coupling to exchanged nucleons.

Fig. 4 a) Simplified diagram for the contact term.

b) Resolution of the nucleon vertex in the diagram a).

Fig. 5 The s-behaviour of $\mathrm{Re}\left(\Gamma_1^1(s)/F_\pi(s)\right)$.

Fig. 6 Comparison of version 1 (dashed line) and version 2 (full line) with the data of ref. [1] and ref. [2]. The curves show $\frac{2}{3}\sigma_{e^+e^-\to\rho\varepsilon}$.

References

1. G. Barbarino et al., Nuovo Cimento Letters 3 (1972) 689
F. Ceradini et al., Phys. Lett. 43 B (1973) 341

2. M.D. Bernardini et al., Phys. Lett. 53 B (1974), 384

3. SLAC-Berkely-Tufts collaboration, H.H. Bingham et al.,
Phys. Lett. B 41 (1972), 635

4. P. Estabrooks and A.D. Martin, Phys. Lett. 53 B (1974), 253
B. Hyams et al., CERN preprint 1975

5. M. Bernardini et al., Phys. Lett 46 B (1973) 261

6. A.C. Hirshfeld and G. Kramer, Nucl. Phys. B 74 (1974), 211

7. B. Schrempp-Otto, F. Schrempp and T. Walsh, Phys. Lett. 36 B (1971) 463
G. Schierholz and K. Sundermeyer, Nucl. Phys. B 40 (1972) 125

8. F. Gutbrod and U. Weiss, Nucl. Phys. B 90 (1975), 52

9. P. Joos et al., Phys. Lett. 52 B (1974) 481

10. G. Kramer and T. Walsh, Z. Physik 263 (1973) 361

11. N. Nakanishi, Graph Theory and Feynman Integrals (Gordon and Breach,
New York, 1971)

12. S. Mandelstam, Proc. Roy. Soc. A237 (1956) 496

13. H. Pilkuhn et al., Nucl. Phys. B 65 (1973), 460

14. G. Köpp, Phys. Rev. D10 (1974), 932

15. Particle Data Group, Phys. Lett. 50 B (1975), 1

16. M. Böhm, H. Joos and M. Krammer, Nucl. Phys. B 69 (1974) 349

17. G. Kramer, G. Schierholz and K. Sundermeyer, DESY 75/30

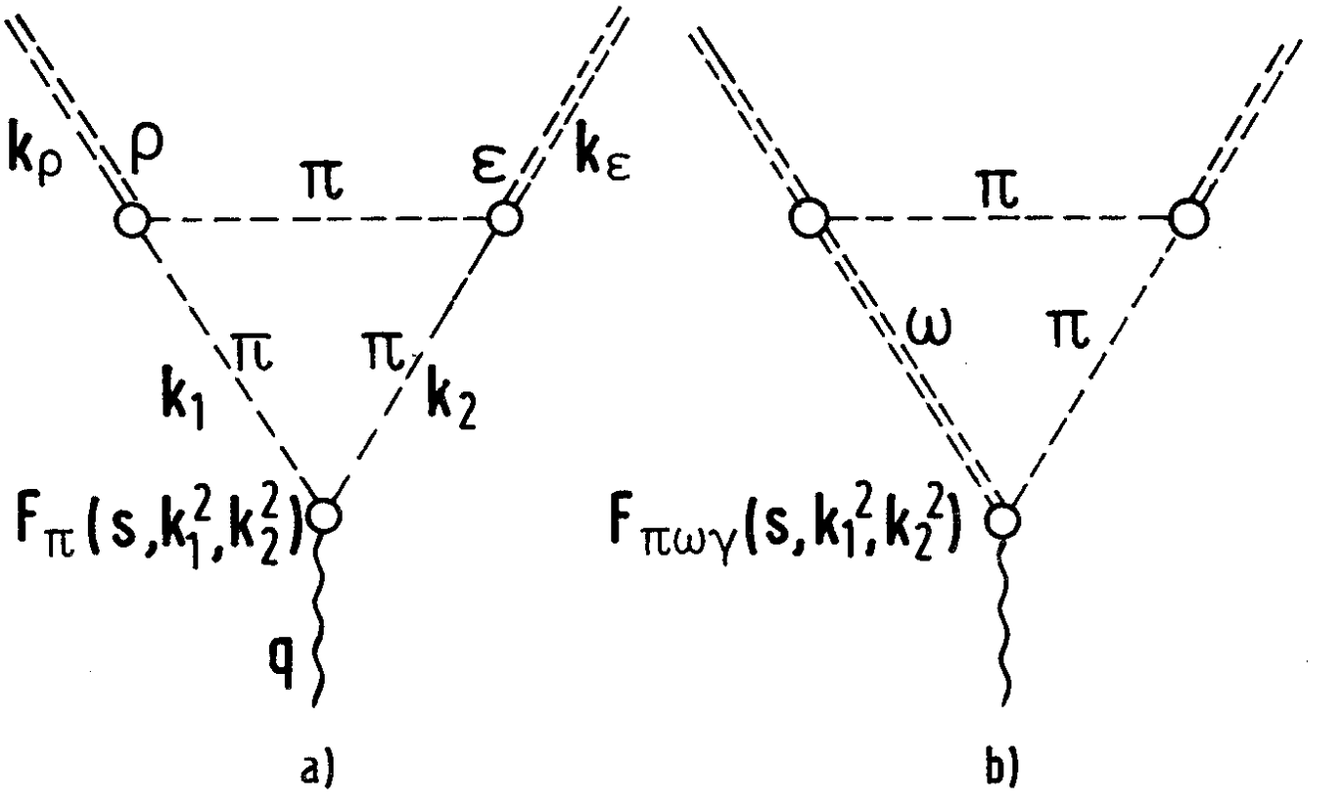
k_ρ
ρ
π
ε
k_ε
π
π
k_1
k_2
$F_\pi(s,k_1^2,k_2^2)$
q
a)
π
ω
π
$F_{\pi\omega\gamma}(s,k_1^2,k_2^2)$
b)

Fig.1

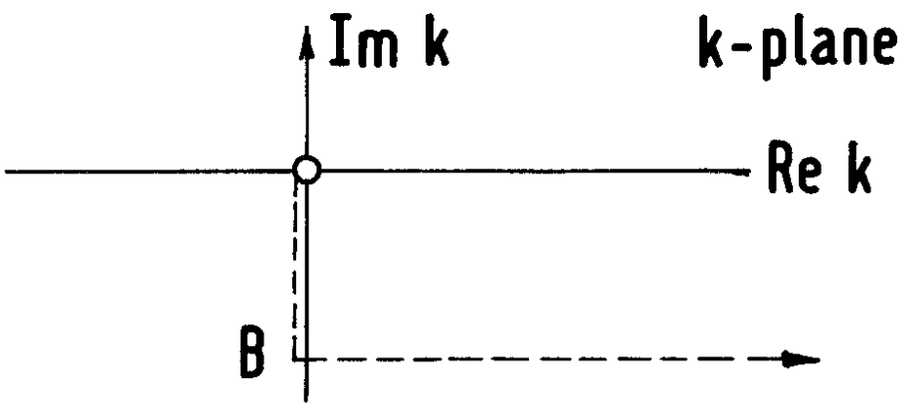
Im k
k-plane
Re k
B

Fig.2

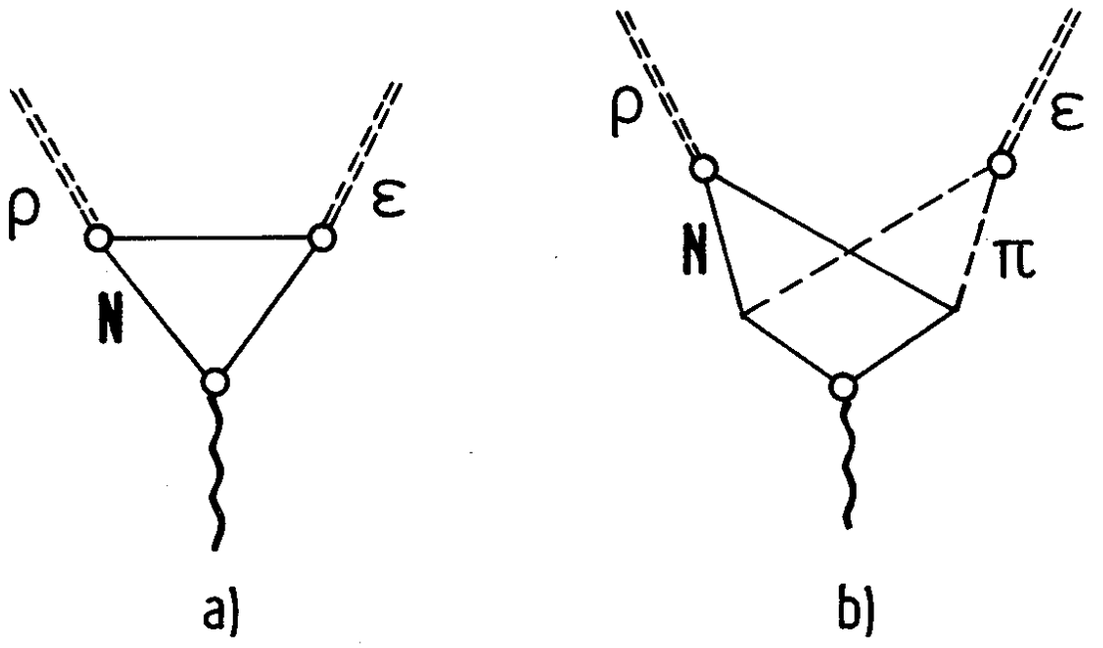

Fig. 3

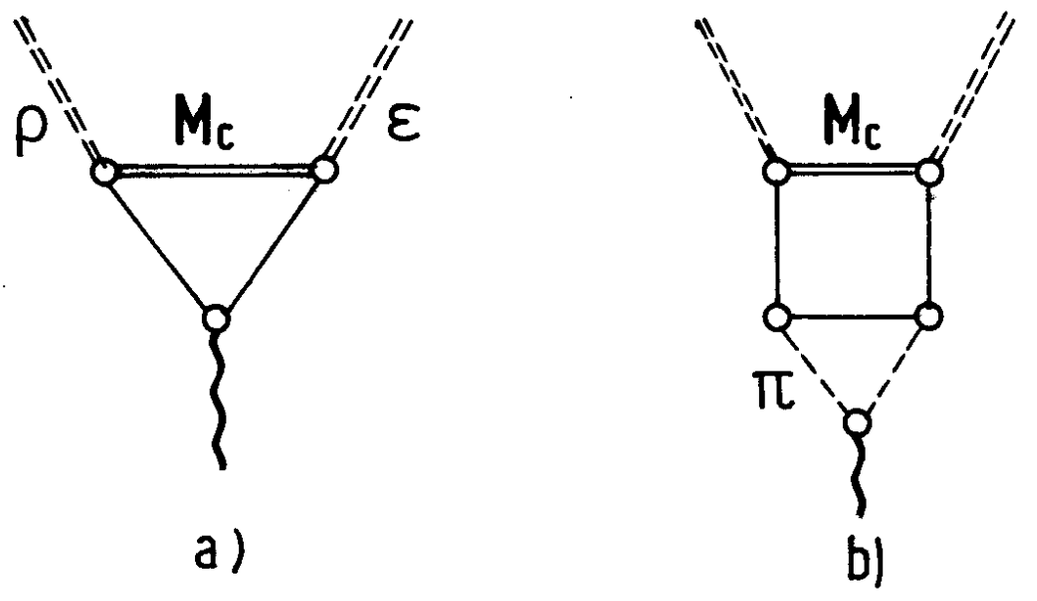

Fig. 4

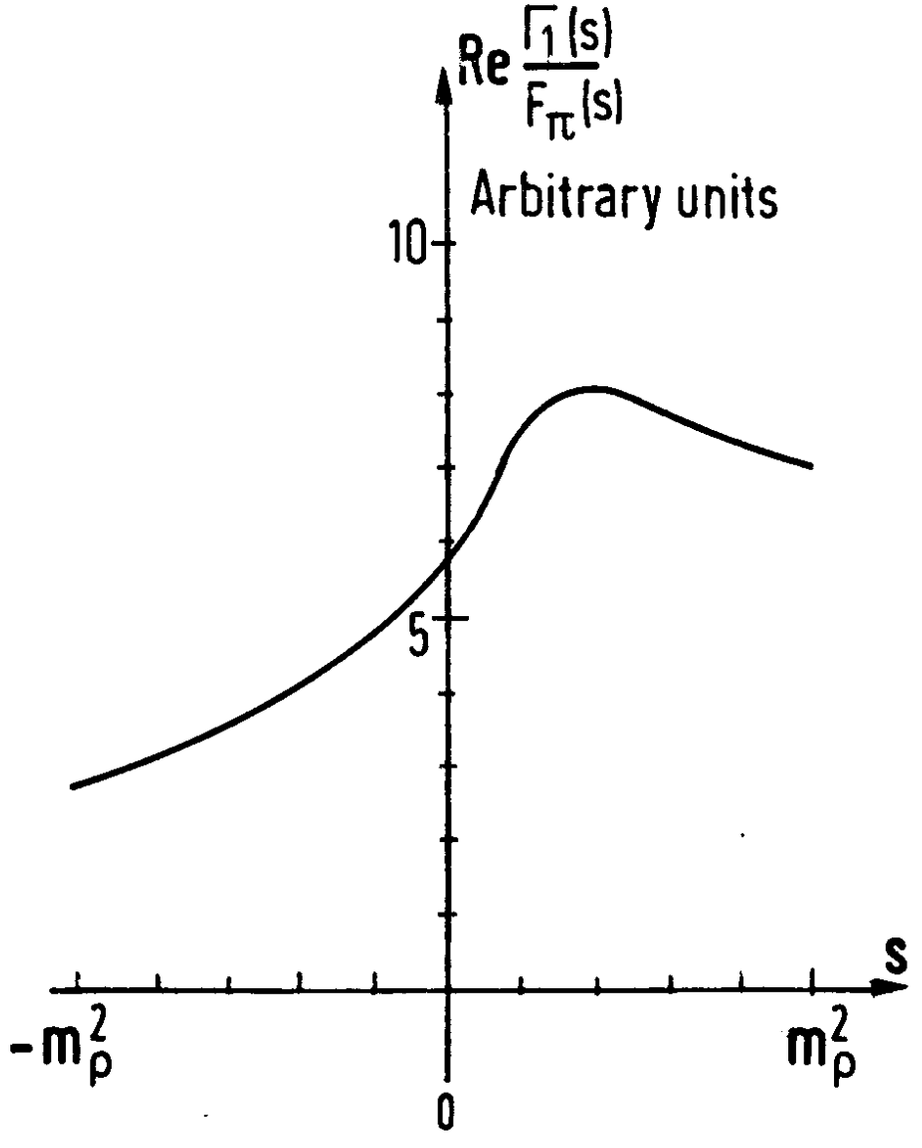
Re $\frac{\Gamma_1(s)}{F_\pi(s)}$
Arbitrary units
10
5
0
s
$-m_\rho^2$
m_ρ^2

Fig.5

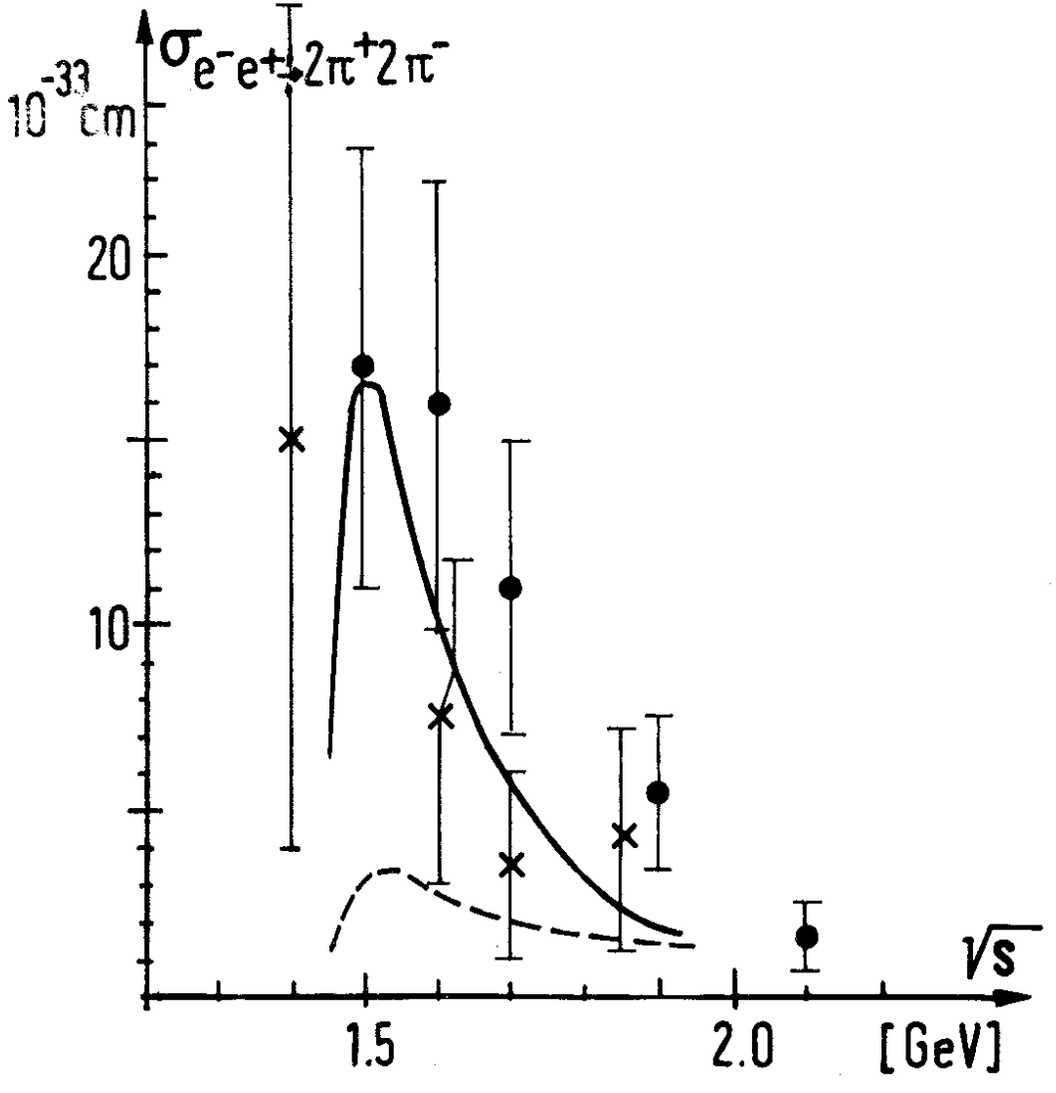
$\sigma_{e^-e^+\to 2\pi^+2\pi^-}$
10^{-33} cm
20
10
1.5
2.0
$\sqrt{s}$
[GeV]

Fig.6